ECINADS-D6.2c: Impact of dynamic SGS models in variational multiscale LES on unstructured grids : application to bluff body flows

Carine Moussaed[a], Stephen Wornom[b],
Maria-Vittoria Salvetti[c], Bruno Koobus[a], Alain Dervieux[d]

[a] *I3M, Université Montpellier 2, Place Eugène Bataillon, 34095 Montpellier cedex, France*
[b] *LEMMA, 2000 Route des Lucioles, 06902 Sophia-Antipolis, France*
[c] *Dipartimento di Ingegneria Aerospaziale,Università di Pisa, Via G. Caruso 8, 56122 Pisa, Italy*
[d]*INRIA, 2004 Route des Lucioles, 06902 Sophia-Antipolis, France*

Abstract

The effects of dynamic subgrid scale (SGS) models are investigated in variational multiscale (VMS) LES simulations of bluff body flows. The spatial discretization is based on a mixed finite element/finite volume formulation on unstructured grids. In the VMS approach used in this work, the separation between the largest and the smallest resolved scales is obtained through a variational projection operator and a finite volume cell agglomeration. The dynamic version of Smagorinsky and WALE SGS models are used to account for the effects of the unresolved scales. In the VMS approach, these effects are only modeled in the smallest resolved scales. The dynamic VMS-LES approach is applied to the simulation of the flow around a circular cylinder at Reynolds numbers 3900 and 20000 and to the flow around a square cylinder at Reynolds numbers 22000 and 175000. It is observed as in previous studies that the dynamic SGS procedure has a smaller impact on the results within the VMS approach than in LES. But improvements are demonstrated for important features like the recirculating part of the flow. The global prediction is improved for a small computational extra cost.

Keywords: variational multiscale LES, dynamic SGS model, unstructured grids, circular cylinder, square cylinder.

1 Introduction

In spite of an extensive research for more than a century applied to the flows in turbulent regime, their modelling remains a big challenge even today. The Direct Numerical Simulation (DNS), which numerically resolves all the significant scales of

motion in a flow down to the Kolmogorov scales, is still not practical for engineering applications. The Large Eddy Simulation (LES) directly computes the large-scale turbulent structures, which are responsible for the transfer of energy and momentum in a flow, while modelling the smaller dissipative and more isotropic structures. Today LES is increasingly used in industrial applications, at least for those flows for which the statiscal approach, which consists in time-averaging the Navier-Stokes (RANS) equations, encounters difficulties in giving accurate predictions. Paradigmatic examples of such flows are bluff-body wakes. A RANS calculation is little dependent on the Reynolds number and little greedy in CPU time, but provides only a limited information. Moreover, RANS modelling presents a strong degree of empiricism, making this approach scarcely reliable for various types of flow. LES is the midway between DNS and RANS modelling as for both the amount of information available from the simulations and the computational costs. A variational multiscale (VMS) formulation of LES has been proposed in [10]. This approach might be effective in obtaining a good compromise between accuracy and computational requirements. The main idea of VMS-LES is to decompose, through Galerkin projection, the resolved scales into the largest and smallest ones and to add the SGS model only to the smallest ones. This is aimed at reducing the excessive dissipation introduced by eddy-viscosity SGS models also on the large scales.

The present work is part of a research activity aimed at developing and validating different approaches to turbulence for the simulation of fluid dynamic problems in an industrial context. In this work, we investigate the effect of employing dynamic SGS models in the VMS-LES approach, used together with an industrial numerical set-up. This industrial numerical set-up, based on a mixed finite-volume/finite-element discretization, is performed on rather coarse unstructured grids as those often used in industrial applications. The VMS approach is particularly attractive for variational numerical methods and unstructured grids, because it is easily incorporated in such formulations [11] and the additional computational costs with respect to classical LES are very low. The used VMS approach is the one proposed in [11], in which the projection operator in the largest resolved scale space is defined through finite-volume cell agglomeration. Two different dynamic eddy-viscosity SGS models are considered viz. the dynamic version [8, 13] of Smagorinsky [27] and Wall-Adapting local Eddy-Viscosity (WALE) models [21]. Very few dynamic VMS-LES simulations have been performed in the past. Mention can be made about the work of Farhat *et al.* [6] in which a variational analog of Germano's identity has been developped within the VMS-LES approach and applied to a prolate spheroid and a forward swept wing, and the work of Gravemeier [7] in which a VMS-LES approach is combined with a dynamic Smagorinsky model for the simulation of a turbulent flow in a diffuser. The classical LES and VMS-LES methodologies have been applied in the past, together with the above mentioned non-dynamic eddy-viscosity models, to the simulation of the flow around a circular cylinder at different Reynolds numbers [24, 23]. In the present paper, we present classical LES and VMS-LES simulations of bluff-body flows carried with the above non-dynamic SGS models as well as with their dynamic counterpart, in order to evaluate the impact of the dynamic procedure on the SGS viscosity and on the simulation results. To this aim we consider

the flow around a circular cylinder at Reynolds numbers 3900 and 20000, and the flow around a square cylinder at Reynolds numbers 22000 and 175000.

2 Variational Multiscale LES approach

The VMS formulation consists in splitting between the large resolved scales (LRS) i.e. those resolved on a virtual coarser grid, and the small resolved ones (SRS) which correspond to the finest level of discretization. The VMS-LES method does not compute the SGS component of the solution, but models its dissipative effects in the SRS, and preserves the Navier-Stokes model for the large resolved scales.

2.1 VMS formulation

In the present work, we adopt the VMS approach proposed in [11] for the simulation of compressible turbulent flows through a finite volume/finite element discretization on unstructured tetrahedral grids. Let V_{FV} be the space spanned by ψ_k, the finite volume basis function and V_{FE} the one spanned by ϕ_k, the finite element basis function. In order to separate large- and small- scales, these spaces are decomposed as: $\psi_k =< \psi_k > +\psi'_k$ and $\phi_k =< \phi_k > +\phi'_k$ where the *brackets* denotes a coarse scale and the *prime* a fine scale. Consequently to this decomposition, the variables of the flow are decomposed as follows:

$$W =< W > +W' + W^{SGS} \tag{1}$$

where $< W >$ are the LRS, W' the SRS and W^{SGS} are the unresolved scales. In [11] , a projector operator based on spatial average on macro-cells is defined in the LRS space to determine the basis functions of the LRS space:

$$< \psi_k >= \frac{Vol(C_k)}{\sum_{j\epsilon I_k} Vol(C_j)} \sum_{j\epsilon I_k} \psi_j \quad ; \quad \psi'_k = \psi_k - < \psi_k > \tag{2}$$

for finite volumes, and

$$< \phi_k >= \frac{Vol(C_k)}{\sum_{j\epsilon I_k} Vol(C_j)} \sum_{j\epsilon I_k} \phi_j \quad ; \quad \phi'_k = \phi_k - < \phi_k > \tag{3}$$

for finite elements. $Vol(C_j)$ denotes the volume of C_j, the cell around the vertex j, and $I_k = \{ j/C_j \in C_{m(k)} \}$ where $C_{m(k)}$ is the macro-cell containing the cell C_k. The macro-cells are obtained by a process known as agglomeration [12]. The SGS model which introduces the dissipative effect of the unresolved scales on the resolved scales is only added to the SRS. Let $\Phi = (\phi^1, \phi^2, \phi^3, \phi^4, \phi^5)$ the test functions for the Navier-Stokes system. Superscripts hold for the components entering in each

equation of the system. We use the notation $\Phi_{234} = (\phi^2, \phi^3, \phi^4)$. The term below is added to the SRS momentum equations

$$\begin{aligned} & \int_\Omega \tau' \cdot \nabla \Phi'_{234} \; d\Omega \qquad \text{with} \\ \tau'_{ij} &= -\mu'_{sgs}(2S'_{ij} - \frac{2}{3} S'_{kk}\delta_{ij}) \\ S'_{ij} &= \frac{1}{2}(\frac{\partial u'_i}{\partial x_j} + \frac{\partial u'_j}{\partial x_i}) \end{aligned} \tag{4}$$

where μ'_{sgs} denotes the viscosity of the SGS model used to close the problem, computed as a function of the smallest resolved scales. Likewise, the term

$$\int_\Omega \frac{C_p \mu'_{sgs}}{Pr_{sgs}} \nabla T' \cdot \nabla \Phi'_5 \; d\Omega \tag{5}$$

is added to the fine scales energy equation. C_p is the specific heat at constant pressure and Pr_{sgs} is the subgrid-scale Prandtl number which is assumed to be constant. To summarize, the extra VMS-LES terms writes:

$$(\mathcal{T}^{LES}(W'), \Phi') = \int_\Omega \tau' \cdot \nabla \Phi'_{234} \; d\Omega \; + \; \int_\Omega \frac{C_p \mu'_{sgs}}{Pr_{sgs}} \nabla T' \cdot \nabla \Phi'_5 \; d\Omega.$$

2.2 SGS viscosities

The SGS terms appearing in the LES equations must be expressed through a SGS model. The most commonly used SGS model in LES is the Smagorinsky model [27] in which the eddy viscosity is defined by

$$\mu_{\text{sgs}} = \overline{\rho} \left(C_{\text{s}} \Delta\right)^2 \left|\widetilde{S}\right| \quad , \tag{6}$$

where Δ is the filter width, C_{s} is the Smagorinsky coefficient and $\left|\widetilde{S}\right| = \sqrt{2\widetilde{S_{ij}}}$. The *overline* denotes the grid filter and the *tilde* holds for Favre averaging, $\tilde{f} = \overline{\rho f}/\overline{\rho}$. The filter width is defined as the third root of the grid element volume. A typical value for the Smagorinsky coefficient is $C_s = 0.1$ that is often used, especially in the presence of shear flow.

The second SGS model we considered is the Wall-Adapting Local Eddy -Viscosity (WALE) SGS model proposed by Nicoud and Ducros [21]. The eddy-viscosity term μ_{sgs} is then defined by:

$$\mu_{\text{sgs}} = \overline{\rho}(C_W \Delta)^2 \frac{(\widetilde{S_{ij}}^d \widetilde{S_{ij}}^d)^{\frac{3}{2}}}{(\widetilde{S_{ij}}\widetilde{S_{ij}})^{\frac{5}{2}} + (\widetilde{S_{ij}}^d \widetilde{S_{ij}}^d)^{\frac{5}{4}}} \tag{7}$$

with $\widetilde{S_{ij}}^d = \frac{1}{2}({g_{ij}}^2 + {g_{ji}}^2) - \frac{1}{3}\delta_{ij}{g_{kk}}^2$ being the symmetric part of the tensor ${g_{ij}}^2 = g_{ik}g_{kj}$, where $g_{ij} = \partial \tilde{u}_i / \partial x_j$. As indicated in [21], the constant C_W is set to 0.5.

In the case of a combination of VMS-LES with either of these two eddy viscosity models, $\widetilde{S_{ij}}$ and $\widetilde{S_{ij}}^d$ need be replaced by S'_{ij} and resp.$(S^d_{ij})'$, computed from the u'_i,u'_j velocity fluctuation components instead of the u_i,u_j velocity components.

2.3 Dynamic model

In their original formulations, the constant (C_s, C_w) appearing in the expression of the viscosity of the Smagorinsky and WALE SGS model (Eqs. 6 and 7 respectively) were set to a constant over the entire flow field. For general inhomogeneous flows, however, the SGS viscosity can significantly vary in space. In the dynamic procedure, this constant is then replaced, according to Germano *et al.* [8], by a dimensionless parameter $C(x,t)$ that is allowed to be a function of space and time. The dynamic approach provides a systematic way for adjusting the model constant in space and time, which is desirable for complex turbulent flows. An interesting and appealing feature of this method is that $C(x,t)$ is dynamically estimated using information from the resolved scales making the model self-tuning. The so-called dynamic model [8] has been further developed [9], [13] over the past several years and has been successfully used to study a variety of complex inhomogeneous flows. After the introduction of the grid filter, denoted by *overline* and *tilde*, a second step in the dynamic model consists in the introduction of a second filter, having a larger width than the grid one, which is called the test-filter and denoted by a *hat*. The test-filter is applied to the grid filtered Navier Stokes equations, then, the subtest-scale stress is defined as

$$M_{ij}^{test} = \widehat{\overline{\rho}\overline{\mathbf{u}_i}\overline{\mathbf{u}_j}} - \left(\hat{\overline{\rho}}\right)^{-1}\left(\widehat{\overline{\rho}\overline{\mathbf{u}_i}}\;\widehat{\overline{\rho}\overline{\mathbf{u}_i}}\right) \tag{8}$$

and its deviatoric part can be written using a Smagorinsky or WALE model, as

$$M_{ij}^{test} - \frac{1}{3}M_{kk}^{test}\delta_{ij} \;=\; -C\hat{\Delta}^2\hat{\overline{\rho}}g(\hat{\tilde{\mathbf{u}}})\hat{\tilde{P}}_{ij} \qquad (C \;=\; {C_w}^2 \; or \; {C_s}^2) \tag{9}$$

with $\hat{\tilde{P}}_{ij} = -\frac{2}{3}\hat{\tilde{S}}_{kk}\delta_{ij} + 2\hat{\tilde{S}}_{ij}$ and where $g(\hat{\tilde{\mathbf{u}}})$ denotes the contribution to the SGS viscosity depending on the gradient velocity that appears in (6) for the Smagorinsky model, and in (7) for the WALE model. The constant C, as originally proposed by Germano *et al.* [8], is assumed to be constant at the subgrid and subtest levels.

Let us now introduce the quantity

$$\mathcal{L}_{ij} = M_{ij}^{test} - \hat{M}_{ij} = \widehat{\overline{\rho}\tilde{\mathbf{u}}_i\tilde{\mathbf{u}}_j} - \left(\hat{\overline{\rho}}\right)^{-1}\left(\widehat{\overline{\rho}\tilde{\mathbf{u}}_i}\widehat{\overline{\rho}\tilde{\mathbf{u}}_i}\right) \tag{10}$$

called the Leonard stress, which is known from a LES computation. In order to determine the constant C, one can relate $\mathcal{L}_{ij}$ to the value obtained using the SGS model (Smagorinsky or WALE). This leads to

$$L_{ij} = \mathcal{L}_{ij} - \frac{1}{3}\mathcal{L}_{kk}\delta_{ij} \;=\; (C\Delta^2)B_{ij} \tag{11}$$

where

$$B_{ij} \;=\; \widehat{\overline{\rho}g(\tilde{\mathbf{u}})\tilde{P}_{ij}} - \left(\frac{\hat{\Delta}}{\Delta}\right)^2 \hat{\overline{\rho}}g(\hat{\tilde{\mathbf{u}}})\hat{\tilde{P}}_{ij}.$$

Equation (11) is a tensorial relationship in one unknown ($C\Delta^2$) which has to satisfy:

$$L_{ij} = (C\Delta^2)B_{ij}. \tag{12}$$

This system of six equations can be contracted using the least squares approach [13]. $(C\Delta^2)$ minimizes the quantity

$$Q = (L_{ij} - (C\Delta^2)B_{ij})^2. \tag{13}$$

Thus, $(C\Delta^2)$ is found by setting $\frac{\partial Q}{\partial (C\Delta^2)} = 0$, from which we derive the value of $(C\Delta^2)$:

$$(C\Delta^2) = \frac{L_{ij}B_{ij}}{B_{pq}B_{pq}} \ . \tag{14}$$

A possible drawback of the dynamic procedure based on the Germano-identity [8] when applied to a SGS model already having a correct near-wall behavior, as the WALE one, is the introduction of a sensitivity to the additional filtering procedure. A simple way to avoid this inconvenient is to have a sensor able to detect the presence of the wall, without a priori knowledge of the geometry, so that the dynamic SGS model adapts to the classical constant of the model, which is equal to 0.5 in the near wall region for the WALE model, and compute the constant dynamically otherwise. We adopt the sensor proposed in [3], having the following expression:

$$SVS = \frac{(\widetilde{S_{ij}}^d \widetilde{S_{ij}}^d)^{\frac{3}{2}}}{(\widetilde{S_{ij}}^d \widetilde{S_{ij}}^d)^{\frac{3}{2}} + (\widetilde{S_{ij}}\widetilde{S_{ij}})^3}. \tag{15}$$

This parameter has the properties to behave like y^{+3} near a solid wall, to be equal to 0 for pure shear flows and to 1 for pure rotating flows.

It should be noticed that the implementation of the dynamic SGS models in our software has been optimized so that the additional cost of the resulting dynamic LES and VMS models, in the case of an implicit time-marching scheme, which is our default option, is less than 1% compared to their non-dynamic counterparts.

3 Numerical discretization

The choice of the numerical discretization will influence in two ways this study. First, we use a numerical scheme for compressible flow which needs to be stabilized by numerical dissipation. It is compulsory that the numerical dissipation does not interfere with the LES model. A particular attention is paid to this issue. Second, the VMS formulation is based on the basis functions of the scheme. We briefly recall now the main features of the numerical scheme. Further details can be found in [4] and in [5].

The governing equations are discretized in space using a mixed finite-volume/finite-element method applied to unstructured tetrahedrizations. The adopted scheme is vertex centered, i.e. all degrees of freedom are located at the vertices. P1 Galerkin finite elements are used to discretize the diffusive terms.

A dual finite-volume grid is obtained by building a cell C_i around each vertex i; the finite-volume cells are built by the rule of medians: the boundaries between

cells are made of triangular interface facets. Each of these facets has a mid-edge, a facet centroid, and a tetrahedron centroid as vertices. The convective fluxes are discretized on this tessellation by a finite-volume approach, i.e. in terms of the fluxes through the common boundaries between each couple of neighboring cells. The unknowns are discontinuous along the cell boundaries and this allows an approximate Riemann solver to be introduced. The Roe scheme [25] (with low-Mach preconditioning) represents the basic upwind component for the numerical evaluation of the convective fluxes. The MUSCL linear reconstruction method ("Monotone Upwind Schemes for Conservation Laws"), introduced by Van Leer [28], is adapted for increasing the spatial accuracy. The basic idea is to express the Roe flux as a function of reconstructed values of W at the boundary between two neighboring cells. Attention has been dedicated to the dissipative properties of the resulting scheme which is a key point for its successful application to LES simulations.The numerical dissipation in the resulting scheme is made of sixth-order space derivatives by using suited reconstructions [4]. Time advancing is carried out through an implicit linearized method, based on a second-order accurate backward difference scheme and on a first-order approximation of the Jacobian matrix [19]. The resulting numerical discretization is second-order accurate both in time and space.

4 Applications

4.1 Circular cylinder test-case, Reynolds number 20000

Simulations for the flow around a circular cylinder are carried out at Reynolds number based on the cylinder diameter, D, and the freestream velocity, equal to 20000. The computational domain is such that $-10 \leq x/D \leq 25$, $-20 \leq y/D \leq 20$ and $-\pi/2 \leq z/D \leq \pi/2$, where x, y and z denote the streamwise, transverse and spanwise directions respectively, the cylinder axis being located at $x = y = 0$. Periodic boundary conditions are applied in the spanwise direction while no-slip conditions are imposed on the cylinder surface. Characteristic based conditions are used at the inflow and outflow as well as on the lateral surfaces. The freestream Mach number is set equal to 0.1 in order to make a sensible comparison with incompressible simulations in the literature. Preconditioning is used to deal with the low Mach number regime. The computational domain is discretized by an unstructured grid consisting of approximately 1.8 million of nodes. The averaged distance of the nearest point to the cylinder boundary is 0.001D, and 100 nodes are present in the spanwise direction near the cylinder, with an approximately uniform distribution. LES and VMS-LES simulations have been carried on this grid for the WALE and the Smagorinsky SGS models in their original formulation as well as in their dynamic version.

First of all, the dynamic procedure has a remarkable effect on the amount of introduced SGS viscosity. In all the considered cases, the SGS viscosity produced in the wake by dynamic SGS models is significantly reduced compared to that given by their non-dynamic counterparts. An example is given in Figures 1 and 2, showing

the instantantaneous iso-contours of μ_{sgs}/μ obtained in the VMS-LES simulations with the non-dynamic and dynamic WALE models respectively.

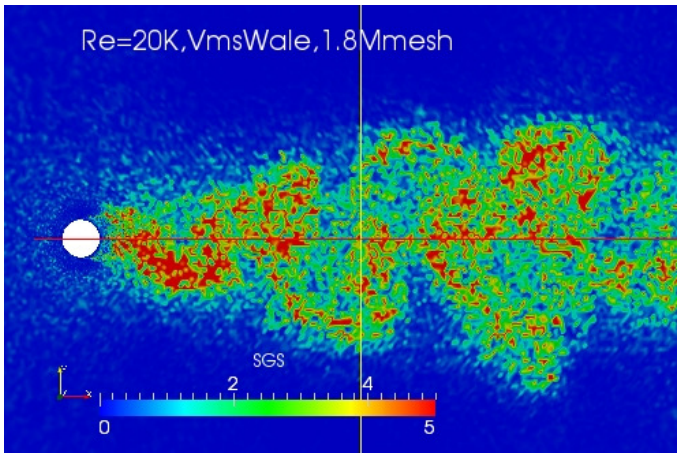

Figure 1: Flow around a circular cylinder at Reynolds 20000 : viscosity ratio for the VMS-WALE.

The impact of these differences in SGS viscosity is investigated in terms of flow bulk parameters and statistics. For all simulations, statistics are computed by averaging in the spanwise homogeneous direction and in time for 30 vortex shedding cycles. The main bulk coefficients are summarized in Table 1. They are compared with the experimental results of [14] and [1] and the review in [22]. As for simulations we recall the LES results of [2], obtained with 2.3 million of cells, and of [26]. From this table, it appears that, except for the Smagorinsky SGS model within the LES approach, the bulk coefficients are in overall good agreement with the available numerical and experimental data. The maximum value of the turbulence intensity for all the simulations carried out is underestimated compared to to the experimental value. This is however not surprising, since as shown also in Figures 1 and 2, the contribution of the SGS model is significant in the very near wake region ($x/D < 2$), which is not taken into account in the computation of the resolved turbulence intensity. From this table, it also appears that the impact of the dynamic procedure within the VMS-LES approach is rather small, and less important than with the LES approach. This can be explained by the fact that in the VMS-LES approach the SGS viscosity only acts on the smallest resolved scales, while this viscosity applies on all the resolved scales in classical LES. This observation is also confirmed by the mean pressure coefficient distribution at the cylinder, as shown in Figure 3 and 4.

A substantial improvement in the prediction of the distribution of the turbulence intensity can nevertheless be observed with the dynamic version of VMS-LES. This distribution along the wake centerline is depicted in Figures 5 and 6 for the non-dynamic and dynamic VMS-LES Smagorinsky respectively. These results are compared with those of Aradag [2] and the experimental data of Lim and Lee [14]. It can be observed the notable improvement brought by the dynamic SGS model

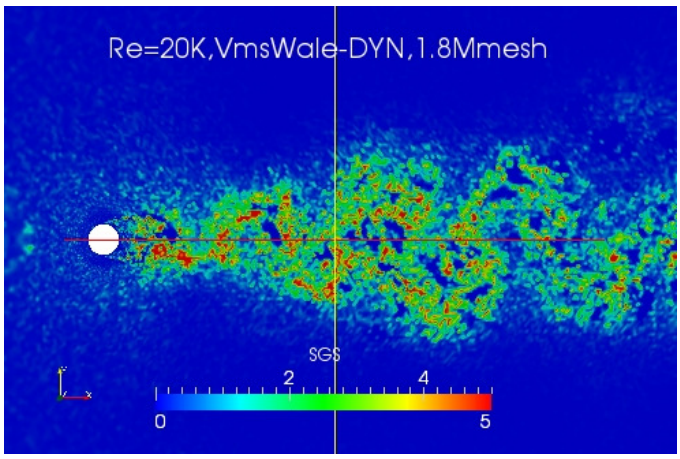

Figure 2: Flow around a circular cylinder at Reynolds 20000 : viscosity ratio for the dynamic VMS-WALE.

	$\overline{C_d}$	C'_L	l_r	$\text{-}\overline{C_{pb}}$	θ	St	Lv	I
LES Smagorinsky	**1.29**	**.59**	**.85**	**1.27**	**85.1**	**.19**	**.71**	**34.**
LES dyn. Smagorinsky	**1.21**	**.45**	**.93**	**1.20**	**83.8**	**.19**	**.96**	**34.5**
LES WALE	**1.16**	**.39**	**.97**	**1.15**	**84.1**	**.20**	**.71**	**31.5**
LES dyn. WALE	**1.19**	**.44**	**.92**	**1.16**	**84.1**	**.20**	**.96**	**31.8**
VMS Smagorinsky	**1.18**	**.43**	**.88**	**1.20**	**83.5**	**.20**	**.90**	**36.6**
VMS dyn. Smagorinsky	**1.19**	**.45**	**.95**	**1.19**	**84.4**	**.19**	**.96**	**31.8**
VMS WALE	**1.17**	**.42**	**.87**	**1.20**	**84.4**	**.20**	**.96**	**33.7**
VMS dyn. WALE	**1.18**	**.43**	**.89**	**1.19**	**84.4**	**.20**	**.96**	**32.8**
LES [26] **min.**	**.94**	**.17**	**.7**	**0.83**	–	–	–	–
max.	**1.28**	**.65**	**.4**	**1.38**	–	–	–	–
LES [2]	**1.20**	–	**.99**	**1.25**	–	–	**.99**	**38.1**
Exp. [14]	**1.16**	–	–	–	–	–	**1.0**	**37.0**
Exp. [1]	**1.20**	–	–	–	–	–	–	–
Exp. [22]	–	**.45**	–	**1.19**	**78**	**.19**	–	–

Table 1: Bulk flow parameters predicted by dynamic and non-dynamic VMS-LES around a circular cylinder at a Reynolds number of 20000. $\overline{C_d}$ holds for the mean drag coefficient, C'_L for the root mean square of lift, l_r is the recirculation length, $\overline{C_{pb}}$ is the mean pressure coefficient at cylinder basis, θ_{sep} is the separation angle, St is the Strouhal number, Lv denotes the x-location of the maximum in the turbulent intensity distribution, I holds for Max. turb. intensity.

and the overall good prediction obtained with this model.

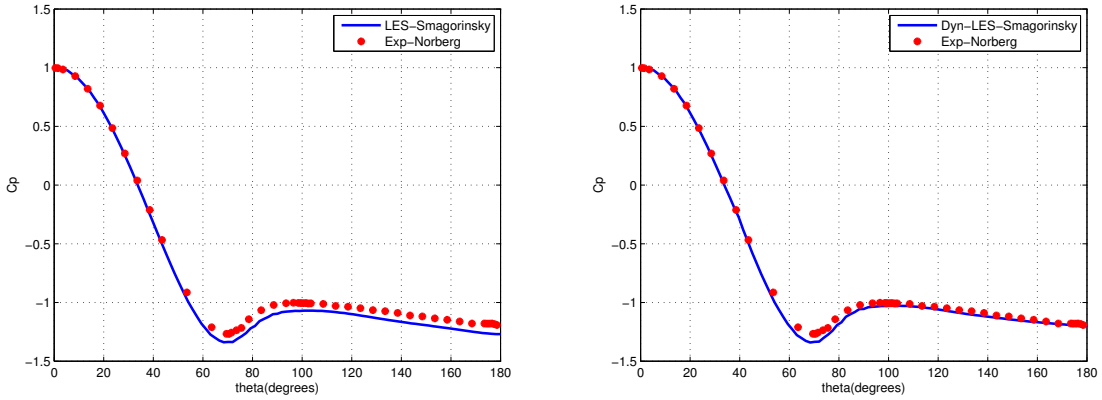

Figure 3: Flow around a circular cylinder at Reynolds 20000 : mean pressure coefficient distribution at the cylinder from the LES Smagorinsky (left) and dyn. LES Smagorinsky (right) computation.

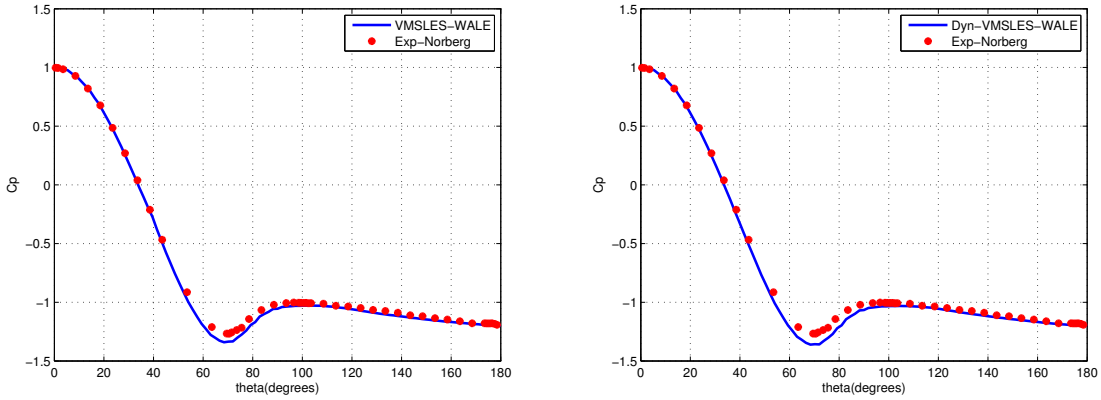

Figure 4: Flow around a circular cylinder at Reynolds 20000 : mean pressure coefficient distribution at the cylinder from the VMS-LES WALE (left) and dyn. VMS-LES WALE (right) computation.

4.2 Cylinder test-case, Reynolds number 3900

In order to confirm that the dynamic procedure has an impact globally rather moderate within the VMS-LES approach, we consider now the flow around a circular cylinder at Reynolds number 3900. The computational domain is the same one used for the test-case Reynolds number 20000. The same boundary and freestream conditions, and the same numerics options, are used than for the previous case. The flow domain is discretized by two unstructured tetrahedral grids. The first one (GR1) contains approximately 290000 nodes, and the averaged distance of the nearest point to the cylinder boundary is 0.017D. The second grid (GR2) is obtained from GR1 by refining in a structured way, i.e. by dividing each tetrahedron in 8,

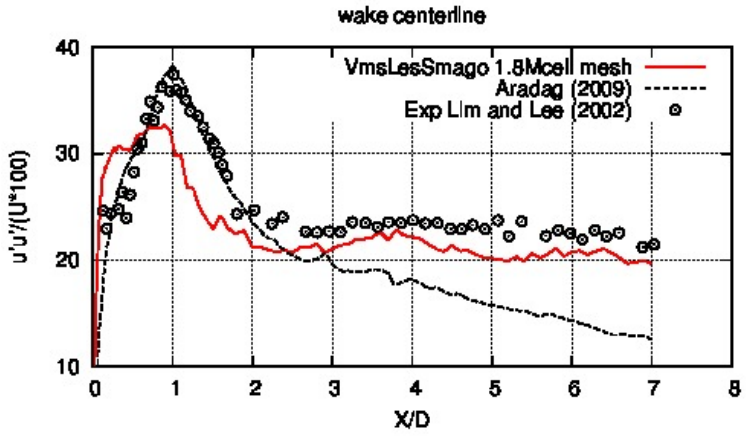

Figure 5: Flow around a circular cylinder at Reynolds 20000 : distribution of the turbulence intensity along the wake centerline from the VMS-LES Smagorinsky computation.

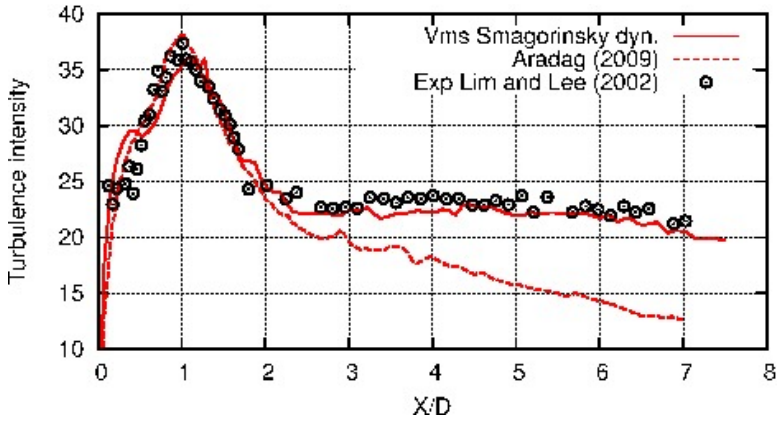

Figure 6: Flow around a circular cylinder at Reynolds 20000 : distribution of the turbulence intensity along the wake centerline from the dynamic VMS-LES Smagorinsky computation.

resulting in approximately 1.46 million of nodes.

The same averaging procedure as for Reynolds 20000 is used in order to compute the statistics. The main bulk coefficients are summarized in Table 2.

One can again notice that the obtained results are in overall good agreement with the experimental data and with other results in the literature. It can also be observed, from some bulk coefficients as the mean drag coefficient, that the impact of the dynamic SGS models is smaller with the VMS-LES approach than with LES, though this is less significant than for Reynolds 20000.

The mean streamwise velocity profile along the wake centerline is reported in Figures 7 and 8 for VMS-LES WALE and its dynamic counterpart on the coarse grid

	$\overline{C_d}$	l_r	$\overline{Cp_b}$	St
LES Smagorinsky (GR1)	**1.05**	**1.00**	**1.05**	**0.21**
LES dyn. Smagorinsky (GR1)	**0.99**	**1.13**	**1.07**	**0.219**
LES WALE (GR1)	**0.98**	**1.09**	**1.04**	**0.22**
LES dyn. WALE (GR1)	**0.94**	**1.13**	**0.99**	**0.22**
VMS Smagorinsky (GR1)	**1.03**	**1.00**	**1.11**	**0.217**
VMS dyn. Smagorinsky (GR1)	**1.01**	**1.05**	**1.08**	**0.219**
VMS WALE (GR1)	**1.00**	**0.96**	**1.10**	**0.22**
VMS dyn. WALE (GR1)	**0.97**	**1.10**	**1.04**	**0.22**
VMS WALE (GR2)	**0.94**	**1.47**	**0.81**	**0.22**
VMS dyn. WALE (GR2)	**0.94**	**1.47**	**0.85**	**0.22**
Exp. Ong-Wallace, min.	–	–	–	**0.205**
max.	–	–	–	**0.215**
Exp. Lourenco-Shi, min.	–	**1.13**	–	–
max.	–	**1.23**	–	–
Exp. Parnaudeau, min.	–	**1.41**	–	**0.206**
= max.	–	**1.51**	–	**0.21**
Exp. Norberg, min.	**0.94**	–	**0.83**	–
max.	**1.04**	–	**0.93**	–

Table 2: Bulk flow parameters predicted by dynamic and non-dynamic VMS-LES around a circular cylinder at a Reynolds number of 3900. Same symbols as previous tables.

(GR1) and the fine grid (GR2) respectively. It can be noted a rather poor prediction obtained on the coarser grid GR1, which is perfectly corrected by the use of the fine grid, and a slight improvement for both grids when the dynamic SGS model is active. This tendancy is confirmed by the prediction of the mean streamwise velocity profile at different streamwise locations depicted in Figures 9 and 10 for the coarse grid and the fine grid respectively. Once again the computation on grid GR2 is much more accurate with a rather sensible improvement provided by the dynamic VMS method for both grids.

4.3 Square cylinder test-case, Reynolds number 22000

Obstacles with square or rectangular sections are extremely frequent in civil engineering structures, like buildings and bridges. The behavior of a flow past such an obstacle is quite different from the one around a circular cylinder. We restrict here to the case of a zero angle of attack.

Even for this case, the simulation is not trivial, although no drag crisis is observed and the flow keeps similar properties for a large interval of Reynolds numbers, from 10000 to 200000. This type of flow is the object of a well-known benchmark [20]

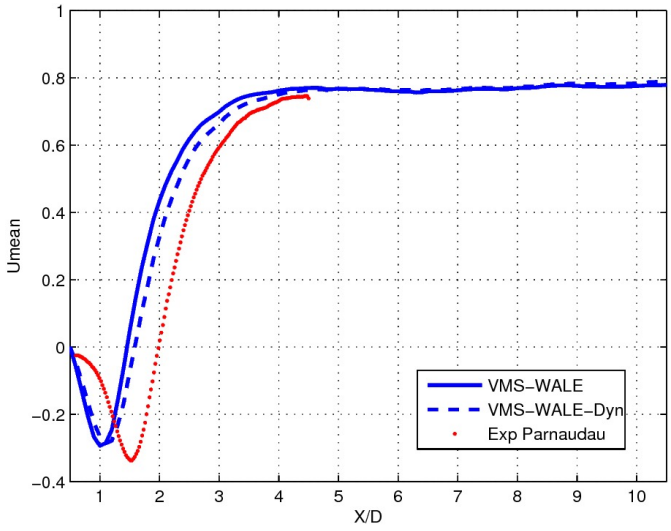

Figure 7: Flow around a circular cylinder at Reynolds 3900 : mean streamwise velocity profile along the wake centerline for VMS-LES WALE and its dynamic counterpart on the coarse grid (GR1).

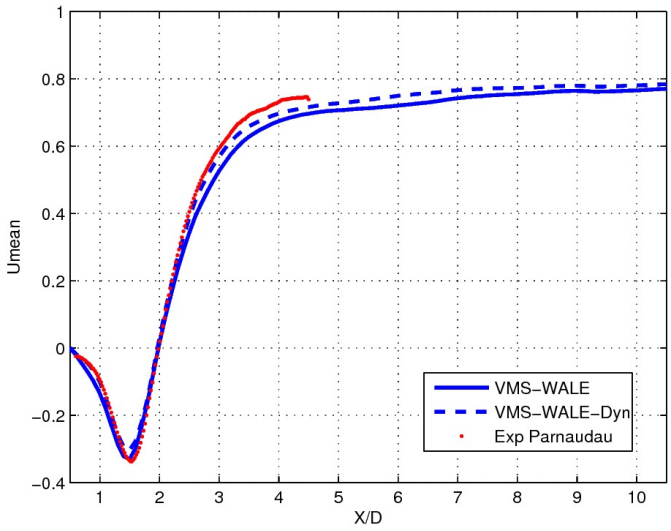

Figure 8: Flow around a circular cylinder at Reynolds 3900 : mean streamwise velocity profile along the wake centerline for VMS-LES WALE and its dynamic counterpart on the fine grid (GR2).

for a Reynolds number of 22000. This section focuses on this case. The overview in [20] points out that, in spite of the fixed separation, this flow is challenging for

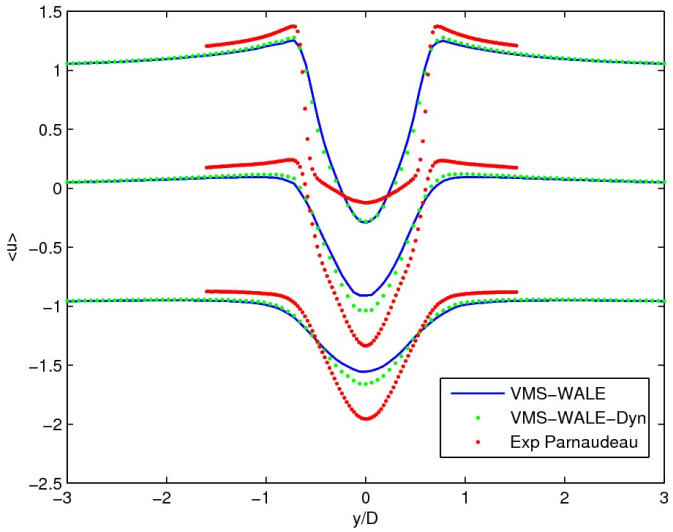

Figure 9: Flow around a circular cylinder at Reynolds 3900 : mean streamwise velocity profile at $x/D = 1.06$ (top), $x/D = 1.54$ (center) and $x/D = 2.02$ (bottom), obtained for VMS-LES WALE and its dynamic counterpart on the coarse grid (GR1).

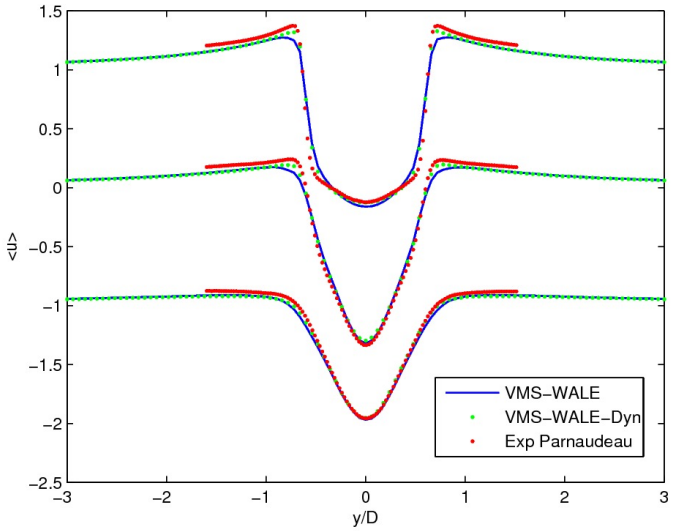

Figure 10: Flow around a circular cylinder at Reynolds 3900 : mean streamwise velocity profile at $x/D = 1.06$ (top), $x/D = 1.54$ (center) and $x/D = 2.02$ (bottom), obtained for VMS-LES WALE and its dynamic counterpart on the fine grid (GR2).

simulations, the main difficulty being the fact that the inflow is basically laminar, and transition takes place in the separate free shear layers on the side of the cylinder.

The mesh involves 1210000 cells and no-slip conditions are applied on the obstacle. Mean properties have been derived from a 30-period computation, using about 20000 time steps.

	$\overline{C_d}$	l_r	St	C_l'	C_d'
VMS Smagorinsky	**2.08**	**0.74**	**0.127**	**1.38**	**0.25**
VMS dyn. Smagorinsky	**2.06**	**0.82**	**0.128**	**1.28**	**0.24**
DNS Verstappen et al.					
1997	**2.09**	–	**0.133**	**1.45**	**0.178**
2010	**2.1**	–	**0.133**	**1.22**	**0.21**
Exp. Lyn et al.	**2.1**	**0.88**	**0.133**	–	–
Exp. Luo, Rey=34 000	**2.21**	–	**0.13**	**1.21**	**0.18**

Table 3: Bulk flow parameters predicted by dynamic and non-dynamic VMS-LES around a square cylinder at a Reynolds number of 22000. Same symbols as previous tables.

In Table 3 we compare a few bulk quantities for our non-dynamic and dynamic calculations with a DNS calculation by Verstappen *et al.*, (from the 1997 paper [29] and from more recent slides) and measurements by Lyn *et al.*, [17, 18], Luo *et al.*, [16].

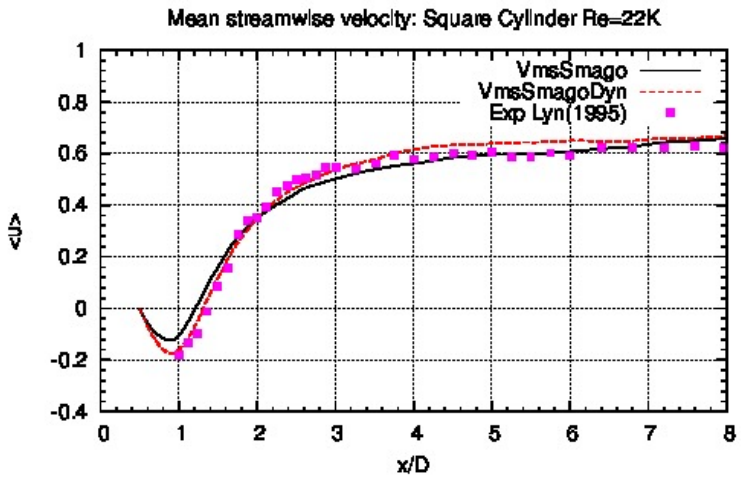

Figure 11: Flow around a square cylinder at Reynolds 22000 : mean horizontal velocity on the centerline of the wake.

Lyn *et al.* and Verstappen *et al.* data can be considered as rather accurate ones, since in good accordance. Also the first drag fluctuation of Verstappen *et al.* and that of Luo *et al.* are in good accordance, but the former author has refered more recently to a higher figure, 0.21, closer to our output. On this experimental and

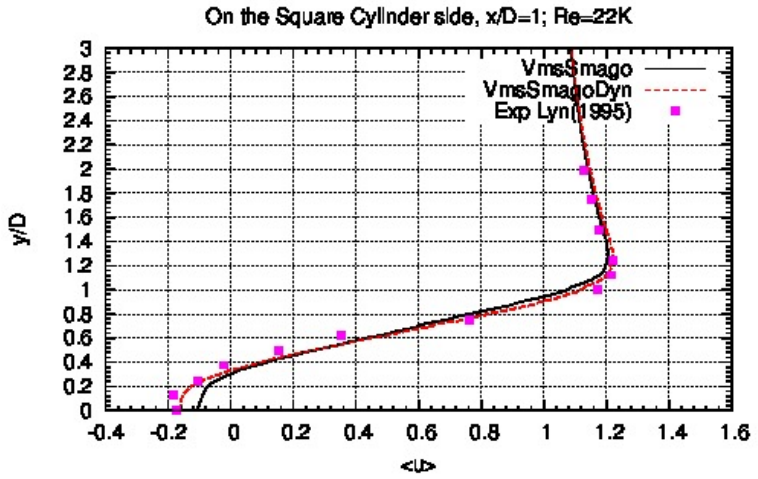

Figure 12: Flow around a square cylinder at Reynolds 22000 : mean horizontal velocity at x/D=1.

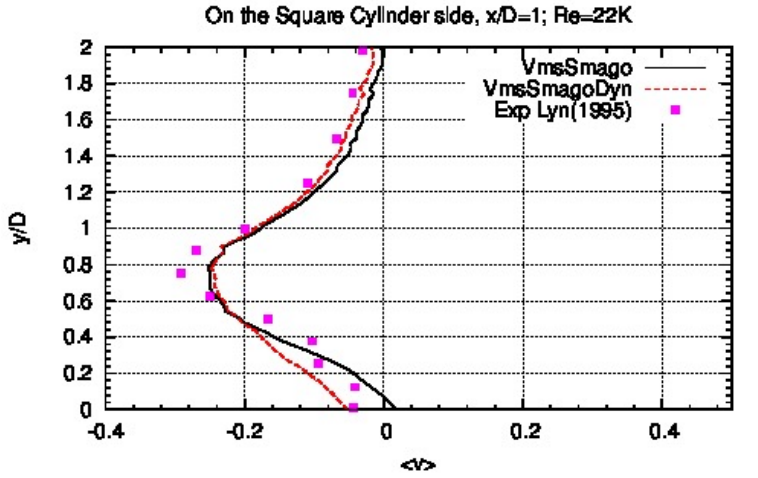

Figure 13: Flow around a square cylinder at Reynolds 22000 : mean vertical velocity at x/D=1.

DNS basis, the accuracy of our computed bulk quantities seems to be in the range 2-7%, with a slight improvement for the combination of VMS and dynamic, except for the rms of the drag. Figures 11-14 show different mean velocity profiles obtained in our VMS-LES simulations with dynamic and non-dynamic Smagorinsky model, compared against the experimental data of Lyn *et al.*.

In particular, Figures 11 and 12 show the profile of the mean streamwise velocity along the centerline of the wake and along the vertical axis at $x/D = 1$, while the profiles of the mean vertical velocity are reported in Figures 13 and 14 at $x/D = 1$ and $x/D = 0$ respectively. The dynamic SGS models generally leads to a better agreement with the experimental data, although the differences with the results

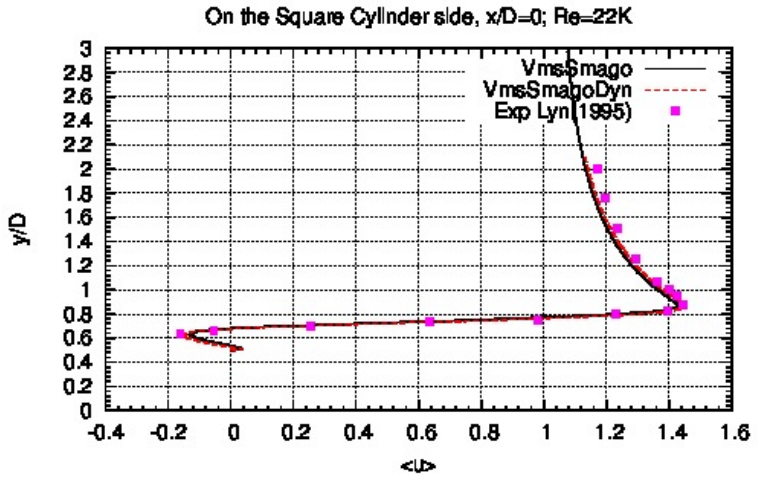

Figure 14: Flow around a square cylinder at Reynolds 22000 : mean vertical velocity at x/D=0.

obtained by the classical Smagorinsky model are rather small.

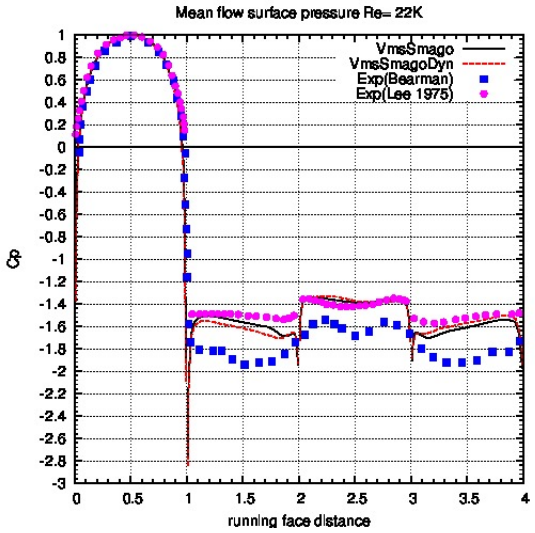

Figure 15: Flow around a square cylinder at Reynolds 22000 : mean pressure coefficient distribution at the cylinder.

As for the mean pressure coefficient distribution at the cylinder, depicted in Figure 15, the results obtained by the dynamic and non-dynamic VMS-LES are close to each other, but do not match with the measurements of Bearman and Obasaju, for which the drag seems far from the Lyn *et al.* and Verstappen *et al.* results. A similar remark was made in [15]. By comparing with the outputs of Lee obtained at Reynolds number 175000, one can notice that a good matching is obtained.

4.4 Square cylinder test-case, Reynolds number 175000

As already mentioned, this higher Reynolds is not expected to produce a very different flow, but to be more difficult to compute. Typically, mean pressure distribution and then mean drag are not supposed to change much, see Table 4. We find a recirculation zone notably shorter than for the smaller Reynolds number case, as expectable, see Figure 16 and Table 4, and compare them with Table 3, but we did not find any result confirming our figure. However, our calculation was not able to predict a lower Strouhal.

In Figure 17, which depicts the instantaneous vorticity field obtained by our calculations, one can notice the higher level of fluctuations produced by the dynamic VMS-LES computation which introduces less SGS viscosity than the non-dynamic counterpart, see for example the shear layer on the upper side of the cylinder.

	$\overline{C_d}$	l_r	St	C'_l	C'_d	C_{pb}
VMS Smagorinsky	**2.03**	**0.73**	**0.129**	**1.29**	**0.26**	**1.30**
VMS dyn. Smagorinsky	**2.03**	**0.75**	**0.127**	**1.26**	**0.23**	**1.30**
Exp. Lee	**2.06**	–	**0.122**	**1.21**	**0.23**	**1.30**
Exp. Vickery	–	–	**0.12**	**1.32**	–	–

Table 4: Bulk flow parameters predicted by dynamic and non-dynamic VMS-LES around a square cylinder at a Reynolds number of 175000. Same symbols as previous tables.

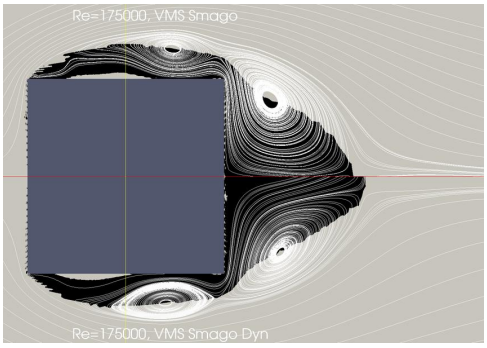

Figure 16: Flow around a square cylinder at Reynolds 175000 : mean vertical velocity of non-dynamic (top) and dynamic (bottom) models. Trajectories and (in black) negative horizontal velocity region.

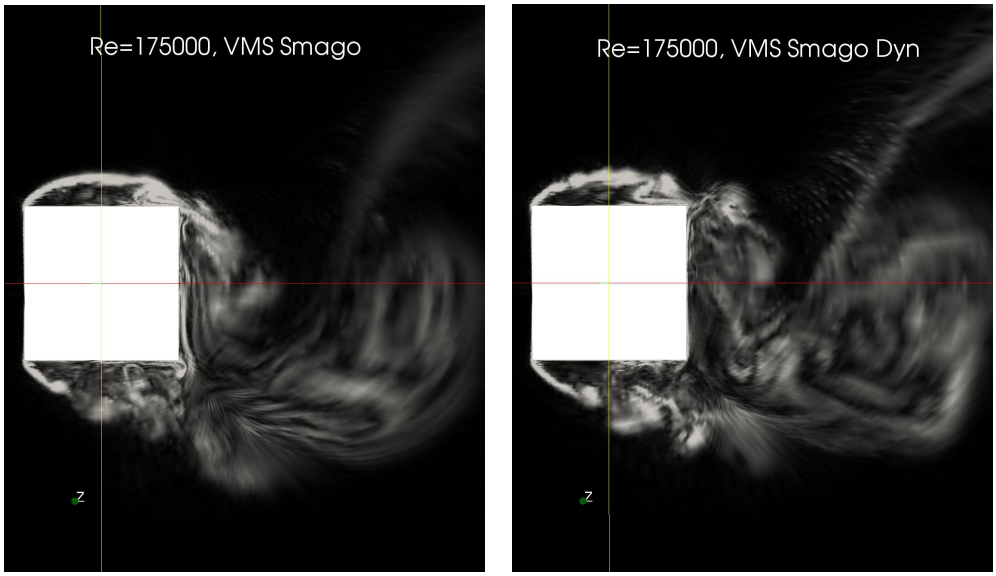

Figure 17: Flow around a square cylinder at Reynolds 175000 : instantaneous vorticity field for VMS-LES Smagorinsky (left) and its dynamic counterpart (right).

5 Conclusion

A variational multiscale LES approach combined with dynamic SGS models has been presented and evaluated for the simulation of bluff body flows in subcritical regimes. While the VMS approach selects which scales are damped by the SGS viscosity, the dynamic procedure selects in which regions a high damping is applied. Somewhat surprisingly, previous works combining both tended to prove that the two methods give similar effects and cannot bring complementary improvements. In this paper we propose a non CPU-costly dynamic version and we re-examine this question by focusing on blunt body flows. More specifically, the simulation of the flow around a circular cylinder at Reynolds numbers 3900 and 20000 and the flow around a square cylinder at Reynolds 22000 and 175000 have been taken as benchmark tests.

The key ingredients of the numerics and modeling used in this work are : unstructured grids, a second-order accurate numerical scheme stabilized by a tunable numerical diffusion proportional to sixth-order space derivatives, and the VMS formulation combined with the dynamic and non-dynamic Smagorinsky and WALE SGS models. A set of rather coarse unstructured grids, as those often used in industrial applications, have been selected in order to get significant deviations between models, while obtaining rather good predictions.

We first verified that, for the different model tested, the bulk coefficients and the main flow features are in overall good agreement with experimental data and other numerical results in the literature.

We observed that the dynamic procedure importantly reduces the amount of dissipation with respect to the non-dynamic one. However, it is observed that,

when combined with the VMS-LES approach, the effect of the dynamic procedure on bulk coefficients and main flow, has a smaller impact on the results than when used with a pure LES, which partly confirms the conclusions of previous works. This may be explained by the fact that the SGS viscosity only acts on the smallest resolved scales in the VMS-LES approach, while this viscosity applies to all the resolved scales in classical LES models.

Nevertheless, an overall improvement is observed with the combination Dynamic-VMS. First, this remark holds for bulk quantities. Second, a notable improvement in the distribution of the turbulence intensity is obtained for the circular cylinder at Reynolds number 20000. Third, the same observation can be made for mean streamwise velocity profiles in the case of the circular cylinder at Reynolds number 3900. Fourth, for the square cylinder at Reynolds number 22000, the examination of mean velocity profiles shows that deviations with respect to measurements in the recirculation zone produced by the non-dynamic VMS-LES model are in most part corrected by its dynamic counterpart.

Acknowledgment

This work has been supported by French National Research Agency (ANR) through COSINUS program (project ECINADS n^o ANR-09-COSI-003). HPC resources from GENCI-[CINES] (Grant 2010-x2010026386 and 2010-c2009025067) are also gratefully acknowledged.

References

[1] J.D. Anderson. *Fundamentals of Aerodynamics*, Second Edition, McGraw-Hill, New York, 1991.

[2] S. Aradag. Unsteady turbulent vortex structure downstream of a three dimensional cylinder, *J. of Thermal Science and Technology*, 29(1):91-98, 2009.

[3] H. Baya Toda, K. Truffin and F. Nicoud. Is the dynamic procedure appropriate for all SGS model. *V European Conference on Computational Fluid Dynamics*, ECCOMAS CFD, J.C.F. Pereira and A. Sequeira (Eds), Lisbon, Portugal, 14-17 June 2010.

[4] S. Camarri, M.V. Salvetti, B. Koobus, and A. Dervieux. A low diffusion MUSCL scheme for LES on unstructured grids. *Comp. Fluids*, 33:1101-1129, 2004.

[5] C. Farhat, B. Koobus and H. Tran. Simulation of vortex shedding dominated flows past rigid and flexible structures.*Computational Methods for Fluid-Structure Interaction*, 1-30, 1999.

[6] C. Farhat, A. Rajasekharan, B. Koobus. A dynamic variational multiscale method for large eddy simulations on unstructured meshes. *Comput. Methods Appl. Mech. Engrg.*, 195 (2006) 1667-1691.

[7] V. Gravemeier. Variational Multiscale Large Eddy Simulation of turbulent Flow in a Diffuser. *Computational Mechanics*, 39(4):477:495, 2012.

[8] M. Germano, U. Piomelli, P. Moin, W.H. Cabot. A Dynamic Subgrid-Scale Eddy Viscosity Model. *Physics of Fluids*, A 3, 1760-1765, 1991.

[9] S. Ghosal, T. Lund, P. Moin and K. Akselvoll. The dynamic localization model for large eddy simulation of turbulent flows. *J. Fluid Mech.*,286:229-255, 1995.

[10] T.J.R. Hughes, L.Mazzei, and K.E. Jansen. Large-eddy simulation and the variational multiscale method. *Comput. Vis. Sci.*, 3:47-59, 2000.

[11] B. Koobus and C. Farhat. A variational multiscale method for the large eddy simulation of compressible turbulent flows on unstructured meshes-application to vortex shedding. *Comput. Methods Appl. Mech. Eng.*, 193:1367-1383, 2004.

[12] M.H. Lallemand, H. Steve, and A. Dervieux. Unstructured multigridding by volume agglomeration : current status. *Comput. Fluids*, 21:397-433, 1992.

[13] D. K. Lilly. A proposed modification of the Germano subgrid scale closure model. *Physics of Fluids A*, 4:633-635, 1992.

[14] H. Lim and S. Lee. Flow Control of Circular Cylinders with Longitudinal Grooved Surfaces, *AIAA Journal*, 40(10):2027-2035, 2002.

[15] Tiancheng Liu, Gao Liu, Yaojun Ge, Hongbo Wu, Wenming Wu. Extended lattice Boltzmann equation for simulation of flows around bluff bodies in high Reynolds number BBAA VI International Colloquium on Bluff Bodies Aerodynamics and Applications, Milano, Italy, July, 20-24 2008

[16] S. C. Luo and MdG. Yazdani and Y. T. Chew and T. S. Lee, Effects of incidence and afterbody shape on flow past bluff cylinders, *J. Ind. Aerodyn.*, 53:375-399, 1994.

[17] D. A. Lyn and W. Rodi The flapping shear layer formed by flow separation from the forward corner of a square cylinder *J. Fluid Mech.* 261:353-316, 1994.

[18] D. A. Lyn, S. Einav, W. Rodi and J-H. Park, A laser-Doppler velocimetry study of ensemble-averaged characteristics of the turbulent near wake of a square cylinder. *J . Fluid Mech.* 304:285-319, 1995.

[19] R. Martin and H. Guillard. A second-order defect correction scheme for unsteady problems. *Comput. and Fluids*, 25(1):9-27, 1996.

[20] W. Rodi, J.H. Ferziger, M. Breuer and M. Pourqui "Status of Large Eddy Simulation: Results of a Workshop" *J. Fluids Engineering*, Transactions of the ASME, 119, 248-262, (1997).

[21] F. Nicoud and F. Ducros. Subgrid-scale stress modelling based on the square of the velocity gradient tensor. *Flow Turb. Comb.*, 62(3):183-200, 1999.

[22] C. Norberg. Fluctuating lift on a circular cylinder: review and new measurements. *J. Fluids Struct.*, 17:57-96, 2003.

[23] S. Wornom, H. Ouvrard, M.-V. Salvetti, B. Koobus, A. Dervieux. Variational multiscale large-eddy simulations of the flow past a circular cylinder : Reynolds number effects. *Computer and Fluids*, 47(1):44-50, 2011.

[24] H. Ouvrard, B. Koobus, A. Dervieux, and M.V. Salvetti. Classical and variational multiscale LES of the flow around a circular cylinder on unstructured grids. *Computer and Fluids*, 39(7):1083-1094, 2010.

[25] P. L. Roe. Approximate Riemann solvers, parameters, vectors and difference schemes. *J. Comp. Phys*, 43:357-371, 1981.

[26] E. Salvatici and M.V. Salvetti, Large-eddy simulations of the flow around a circular cylinder: effects of grid resolution and subgrid scale modeling, *Wind & Structures*, 6(6):419-436, 2003.

[27] J. Smagorinsky, General circulation experiments with the primitive equations. *Month. Weath. Rev.*, 91(3) :99-164, 1963.

[28] B. Van. Leer. Towards the ultimate conservative scheme. IV :A new approach to numerical convection. *J. Comp. Phys.*, 23:276-299, 1977.

[29] R.W.C.P. Verstappen and A.E.P. Veldman, Direct numerical simulation of turbulence at lower costs. *Journal of Engineering Mathematics* 32:143159, 1997.